Accuracy of the Michaelis-Menten approximation when analysing effects of molecular noise

Michael J. Lawson[1,], Linda Petzold[2], Andreas Hellander[2,*]

January 21, 2015

[1] *Department of Cell and Molecular Biology, Uppsala University, Box 337, SE-75105, Uppsala, Sweden*
[2] *Department of Computer Science, University of California Santa Barbara, Santa Barbara, CA 93106-5070, USA*
[3] *Department of Information Technology, Uppsala University, Box 337, SE-75105, Uppsala, Sweden*

[*] *To whom correspondence should be addressed. E-mail: andreas.hellander@it.uu.se*

Abstract

Quantitative biology relies on the construction of accurate mathematical models, yet the effectiveness of these models is often predicated on making simplifying approximations that allow for direct comparisons with available experimental data. The Michaelis-Menten approximation is widely used in both deterministic and discrete stochastic models of intracellular reaction networks, due to the ubiquity of enzymatic activity in cellular processes and the clear biochemical interpretation of its parameters. However, it is not well understood how the approximation applies to the discrete stochastic case or how it extends to spatially inhomogeneous systems. We study the behaviour of the discrete stochastic Michaelis-Menten approximation as a function of system size and show that significant errors can occur for small volumes, in comparison with a corresponding mass action system. We then explore some consequences of these results for quantitative modelling. One consequence is that fluctuation-induced sensitivity, or stochastic focusing, can become highly exaggerated in models that make use of Michaelis-Menten kinetics even if the approximations are excellent in a deterministic model. Another consequence is that spatial stochastic simulations based on the reaction-diffusion master equation can become highly inaccurate if the model contains Michaelis-Menten terms.

1 Introduction

As the effectiveness of quantitative modelling in biology, on scales ranging from molecular dynamics to well-mixed deterministic models, results in its widespread use, questions have arisen about how to accurately translate a given model from one scale to another [11]. An important finding in molecular systems biology has been the significant role of noise that arises from the discrete and sometimes small number of molecules in intracellular systems. A simplifying model that has been essential in quantifying enzymatic activity is the Michaelis-Menten (MM) approximation [13], which is so fundamental that it is taught as basic biochemistry theory [14]. As an example of the possible effects of molecular noise, it has been shown that the concavity of the Michaelis-Menten propensity function (or convexity of its inhibitory form) can lead to deviation of the mean of a stochastic system from the deterministic signal, an effect referred to as stochastic focusing [15].

Given a deterministic model, it is often of interest to transition it to a discrete stochastic setting to study the potential effects of molecular fluctuations. The Markov process is a popular modelling framework on the discrete stochastic level. Models of stochastic chemical kinetics in this framework can be simulated using the stochastic simulation algorithm (SSA) or one of its many optimised or approximate variants [4]. The original formulation of the model allows for second order mass-action kinetics, but due to the omnipresence of MM terms in models, recent efforts have gone toward deriving conditions for the MM approximation's validity in the discrete stochastic setting [12, 16, 17], with the conclusion that the MM approximation is accurate in the stochastic case provided that the deterministic validity conditions are satisfied. Some work has gone into comparing more generalised approximations [9], but these lack the interpretation and wide use of the MM approximation.

In the classical analysis of MM kinetics, one considers a pool of substrate molecules, whose concentration do not change appreciably during the timescale of the simulation, being converted to product. In this work we present an analysis of a slightly different situation: we consider the flux through a substrate conversion reaction with a Poissonian influx of substrate and an exponential decay of product. This framework closely captures the modeling situation of an enzymatic step embedded in a larger biochemical network. We then focus on the scenario where a modeller begins with a deterministic model in concentration form and transitions it to a discrete stochastic setting. In doing so, it is necessary to introduce a new model parameter, the system volume, in order to convert from concentrations to discrete molecular populations. We show that the choice of this volume, in relation to the other model parameters, can be critical to the accuracy of the simulations. Both the importance of noise, as quantified by the stochastic focusing effect, and the size of the error due to the MM approximations grow quickly with small volume size. In the first part of this paper, we use moment equations to derive an expression for this error as a function of the system size. As we will see, the error introduced by using the MM approximation is only small if the system size is large enough, or equivalently, if the impact of noise on the network is small enough.

We then consider the next logical model progression: the transition from a discrete stochastic well-mixed model to a spatial stochastic model via the reaction-diffusion master equation (RDME). We demonstrate that the dependence of the MM approximation error on volume has important implications for its use in this setting. Spatial inhomogeneity and the importance of locality of reactions in cellular systems often require that the effective reaction volume be very small. Thus the error in the MM approximation can have very large consequences for both diffusion limited and reaction limited systems. Notably, the error depends strongly on the discretisation and increases rapidly with increased spatial resolution. For this reason, the use of MM kinetics in RDME models is highly questionable.

In summary, this paper paints a rather negative picture of the use of MM kinetics for quantitative modelling on the discrete stochastic level. In a well mixed system, as the importance of noise on the network increases, so does the error, making any interpretation of the effects of noise uncertain, especially when the motif is embedded in a larger network that can respond non-linearly to the introduced errors. When transitioning the well mixed model to a spatial setting, this same effect shows up as a discretisation artefact that is likely to render the simulation output highly inaccurate compared to the corresponding mass-action system, irrespective of whether the system is reaction or diffusion limited.

2 Results

2.1 Michaelis–Menten kinetics

We consider the following simple model of enzyme kinetics where substrate S is being created with rate μ and converted to product P by enzyme E

$$\begin{aligned} \emptyset &\xrightarrow{\mu} S \\ E + S &\underset{k_2}{\overset{k_1}{\rightleftharpoons}} ES \xrightarrow{k_3} E + P \\ P &\xrightarrow{k_d} \emptyset. \end{aligned} \tag{1}$$

The birth (inflow) of S and death (outflow) of P ensures that the system reaches non-trivial steady-state levels. This model set-up differs slightly from most of the literature on the validity of Michaelis-Menten kinetics [12, 16, 18], where both μ and k_d are usually taken to be 0, and where the system is initialised with an excess of S. In that case, the kinetics of the transient dynamics of substrate conversion to product is the output of interest. Here, we are interested in the scenario where the motif (1) is part of a larger model, which is a more common setting in quantitative modelling in molecular systems biology. The creation of S by a Poisson process and the exponential decay of P can be seen as a stand-in for the connection with other subsystems of a larger model. For this reason, we consider parameters $\mu > 0$ and $k_d > 0$ so that we obtain a flux through the enzymatic reaction. In this case, the system (1) has a non-trivial steady state under some further assumptions on the model parameters. In what follows, we ask how accurately this steady state can be captured by the corresponding Michaelis-Menten model reduction

$$\begin{aligned} \emptyset &\xrightarrow{\mu} S \\ S &\xrightarrow{V_{max}q[S]} P \\ P &\xrightarrow{k_d} \emptyset, \end{aligned} \tag{2}$$

where $q = \frac{1}{K_m+[S]}$, $K_m = (k_2 + k_3)/k_1$, and $V_{max} = k_3[E_T]$ [14].

The Michaelis-Menten approximation effectively reduces the three reactions in the enzymatic conversion step to a single unimolecular reaction. While this can be advantageous from a computational standpoint [22], a more central reason for its widespread use is the relative ease with which one can interpret and determine (*in vitro*) values for K_m and V_{max}. In contrast, determining the rate constants k_1, k_2 and k_3 of the full model (1) can be quite challenging.

Provided $V_{max} > \mu$, the deterministic ODE models corresponding to (1) and (2) (see, Eqs. (20) and (21)) have unique steady-state solutions that agree for all combinations of the parameter values

$$[S] = \frac{\mu K_m}{\alpha}, \tag{3}$$

where

$$\alpha = V_{max} - \mu, \quad \alpha > 0. \tag{4}$$

For $\alpha < 0$ the inflow rate of substrate is greater than the maximal conversion rate at saturation, so the substrate pool will grow unboundedly. Even though the steady-state for the two models agree for all values of the parameters, the Michaelis-Menten approximation does not necessarily provide an accurate representation of the transient kinetics of (1). In the deterministic case, a validity condition that guarantees a good approximation also for the transient behaviour can be formulated as [17, 18]:

$$[E_T] << [S_0] + K_m, \tag{5}$$

where $[E_T]$ is the total enzyme concentration and $[S_0]$ is the initial substrate concentration.

The Michaelis-Menten model was originally developed to study enzyme kinetics in test tube conditions. An important observation in cellular biology is that *in vivo* kinetics on this scale are more accurately described by discrete stochastic models [12, 16, 17]. A natural question then becomes whether the Michaelis-Menten approximation can be accurately carried over to well-mixed stochastic simulations. This issue was addressed recently by Sanft et al., who suggested that under the same validity condition (5) with concentrations replaced by copy number and the macroscopic rates properly converted to mesoscopic rates, the Michaelis-Menten approximation to (1) with $\mu = 0$ and $k_d = 0$ holds also in well-mixed stochastic simulations.

Introducing the system volume Ω, the propensity function for the conversion reaction $S \to P$ in the well-mixed discrete stochastic case can be written

$$a(S) = \frac{V_{max}S}{K_m + S/\Omega}, \tag{6}$$

where Ω is the system volume. Throughout the paper all rate constants will have the ODE form and will be converted to reaction propensity constants by explicitly multiplying or dividing by Ω as appropriate. The question of how the stochastic MM steady-state solution of (2) compares to the ODE solution in small reaction volumes was addressed in [5] where it is shown that significant deviations can be expected. Depending on the perspective, this deviation can be seen as a breakdown of the MM equations due to intrinsic noise [5], or as a potentially biologically meaningful effect of noise, i.e. stochastic focusing [15]. When we consider the discrete stochastic MM model as an approximation of the discrete stochastic mass action (MA) system, we can regard the stochastic focusing in the MA system as the true effect of noise and compare it to predictions of the MM equations under the influence of noise. As we will see, depending on the system volume Ω, the steady-state solutions of the MA and MM models (1) and (2) may not agree well in a discrete stochastic simulation, even if condition (5) is satisfied in the deterministic setting. More importantly, we will show that the error is significant when the true effect of noise on the system is significant.

2.2 The accuracy of stochastic Michaelis-Menten approximation degrades for small system volumes

As we have seen, the steady-state concentration of S (3) is the same for both the Michaelis-Menten and mass-action systems in the continuum ODE model, independent of the system volume. This is no longer the case in a discrete stochastic setting. Figure 1 shows steady-state concentrations based on solutions of the chemical master equation (CME) (see Methods Eq. (22)) (solid blue and dashed red lines) for varying system volumes Ω. In the thermodynamic limit $\Omega \to \infty$, both CME solutions converge to the ODE solution. By reducing the volume, the system is made increasingly noisy relative to the mean. As can be seen, the Michaelis-Menten and mass-action solutions diverge as Ω is reduced. As expected, both the stochastic mass-action and stochastic Michaelis-Menten steady-state levels increase relative to the ODE solution, but they do not increase at the same rate.

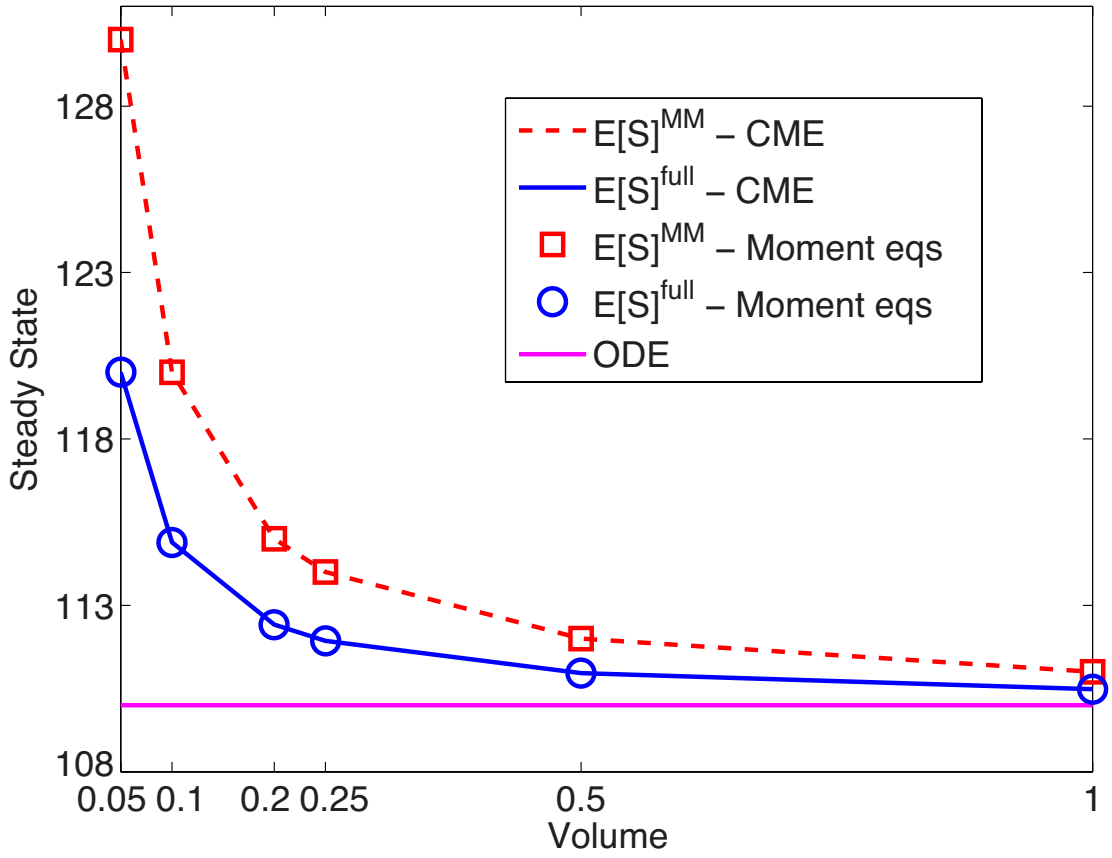

Figure 1: **Steady state concentration of substrate:** Steady state concentration of substrate for the Michaelis-Menten system is shown for different system volumes by solving the CME (dashed red) and by solution of moment equations (8) (red squares). The corresponding CME solutions for the MA reaction system is shown in solid blue and the solution from the moment equations (10) is indicated by blue circles. The solution to the deterministic ODE system (solid magenta) is shown as a reference. As the size of the system is reduced, the concentration of S increases in both discrete stochastic models compared to the ODE model, but not by the same amount. (values used: $\mu = 10\text{mol}s^{-1}$,$k_1 = 0.1\text{mol}^{-1}s^{-1}$, $k_2 = 10s^{-1}$, $k_3 = 1s^{-1}$ and $k_d = 0.2s^{-1}$).

The fact that the steady state of the discrete stochastic MM system deviates from that of the continuous MM system for small volumes, and hence for a large noise level relative to the mean, should not be surprising.

We illustrate the effect intuitively in Fig. 2 where the black solid line shows the reaction propensity (6) as a function of S. Replacing S in (6) with $E[S]$ (blue square), i.e. using a deterministic input, the propensity function takes the value $a(E[S])$ (blue diamond). But for a stochastic system the average rate of the conversion of S depends on the shape of the probability distribution of S (solid blue) and the mean value of the propensity. Hence the average conversion rate of substrate (red diamond) is not the same as the rate obtained by using the mean of S. This effect has previously been described as stochastic focusing [15] in the systems biology context. Mathematically, it is explained by Jensen's inequality applied to random variables

$$E[a(S)] \leq a(E[S]), \tag{7}$$

where a is a concave function (the inverse relationship holds for convex functions).

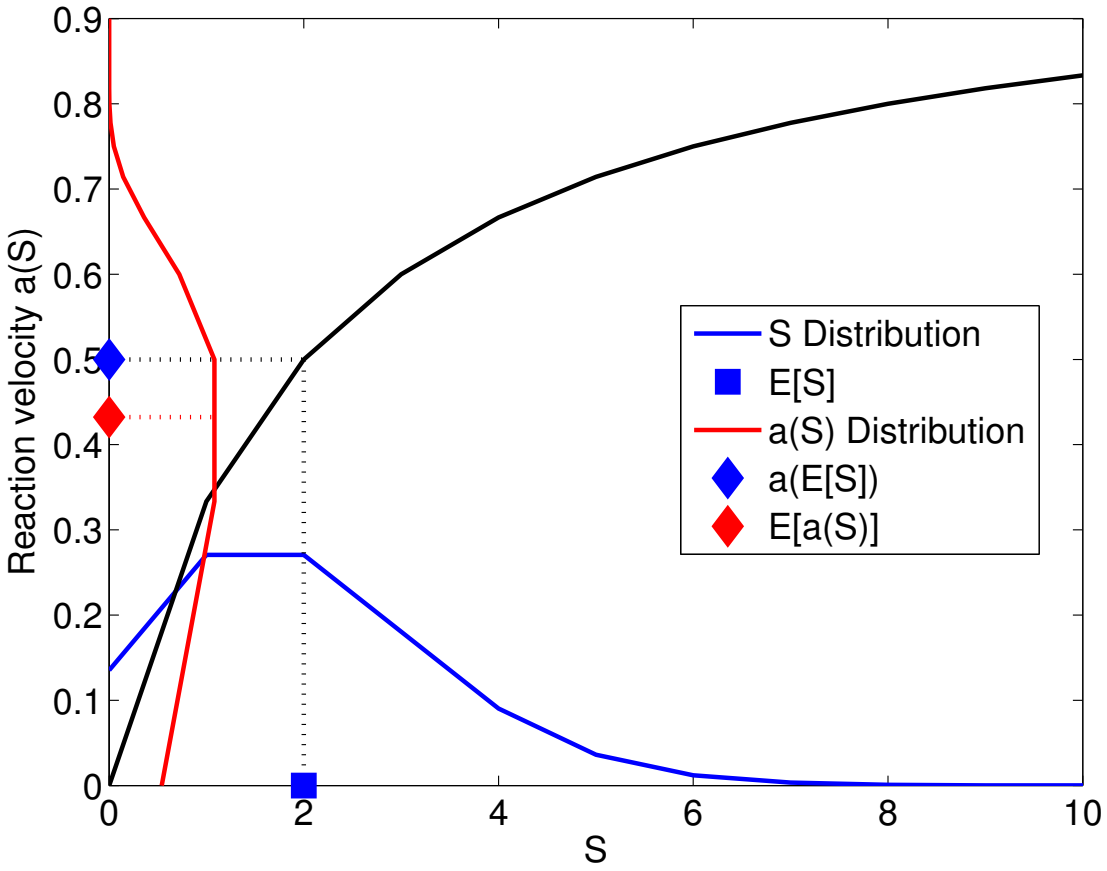

Figure 2: **Effect of Michaelis-Menten approximation on stochastic input:** The black line shows the reaction propensity [6] as a function of substrate population S, for a Michaelis-Menten system (2) with Km = 2 and Vmax = 1. The substrate population S is defined by a Poisson distribution with rate $\lambda = 2$, shown in blue. The mean, $E[S]$, of this population is 2 (blue square) and the reaction velocity for the mean input is 0.5. However, the expected value of the reaction velocity is $\sim 14\%$ lower, leading to higher steady state values of S for the stochastic version of the system (2) compared to the deterministic version.

Clearly, the same type of focusing effect will occur also in the corresponding discrete stochastic mass-action system (1), but not necessarily to the same extent. For both mass action and Michaelis-Menten the strength of this focusing effect depends on the system size. While the discrepancy between the stochastic mass action system (solid blue) and the deterministic system (magenta line) in Fig. 1 can be viewed as a focusing effect caused by molecular noise, the deviation between the stochastic Michaelis-Menten (red curve) and

the stochastic mass action system (blue curve) represents the modelling error due to the Michaelis-Menten approximation. Next we seek analytical estimates for this error.

2.3 Michaelis-Menten Approximation Error

In order to understand this observed discrepancy between the Michaelis-Menten and mass-action models, we write equations for the first and second moments of S [1] (see Eq. (23) in Methods). The steady-state solution of (23) is given by

$$\begin{aligned} E[S]^{MM} &= \Omega\frac{\mu K_m}{\alpha} + \frac{\mu}{\alpha} \\ \sigma^2[S] &= \frac{\mu(\mu + K_m\Omega V_{max})^2}{K_m\Omega V_{max}\alpha^2}, \end{aligned} \tag{8}$$

where the expected values for the discrete stochastic system are expressed in molecular populations. The solution is shown in Fig. 1 (red squares) and it agrees well with the corresponding CME solution. Note that the expected value of substrate may be far from that of the continuum model for small system volumes. As an immediate consequence of (8), in order for the mean steady-state levels in the discrete stochastic case to be close to those in the ODE case, we must require that

$$\Omega K_m >> 1. \tag{9}$$

Note the relationship between this condition and the expression for the range of deviations between the discrete stochastic Michaelis-Menten system at steady state and the deterministic counterpart derived by Grima based on the LNA in [5, Eq. 13]. There, it is shown that the deviation Λ from the ODE solution behaves like $1 < \Lambda < 1 + (\Omega K_m)^{-1}$.

Equations for the first and second moments of the full mass-action system (1) are given in the Methods section (Eq. (24)). The steady state solution for the expected value of substrate S for the full mass action system is given by

$$\begin{aligned} E[S]^{full} =& \Omega\frac{\mu K_m}{\alpha} + \frac{\mu}{2\alpha} - \Omega\frac{V_{max}K_m}{2\alpha} - \Omega\frac{\alpha E_T}{2V_{max}} \\ &+ \frac{1}{\alpha}\sqrt{K_m\mu^2\Omega + \frac{1}{4}\left(V_{max}K_m\Omega + \frac{\alpha^2 E_T\Omega}{V_{max}} - \mu\right)^2}. \end{aligned} \tag{10}$$

We can now define the error in the expected value of the concentration of S due to the MM approximation as

$$\epsilon = \frac{E[S]^{MM}}{\Omega} - \frac{E[S]^{full}}{\Omega}. \tag{11}$$

It is instructive to study the error in the limits of large and small system size. In the large system limit when $\Omega \to \infty$, the two discrete stochastic models agree with each other and with the ODE model

$$\lim_{\Omega\to\infty}\frac{E[S]^{MM}}{\Omega} = \lim_{\Omega\to\infty}\frac{E[S]^{full}}{\Omega} = \frac{\mu K_m}{\alpha}. \tag{12}$$

In the small volume limit $\Omega \to 0$, we can expand (10) around Ω in a Taylor series, truncate higher order terms and obtain an asymptotic expression for the error (see Methods (27)). However, an issue with taking this limit in the discrete stochastic context is that for some positive Ω, $E_T < 1$. This clearly does not make sense in a discrete stochastic model. Indeed, the volumes in Fig. 1 are chosen such that we always have integer numbers of E_T, with the smallest value corresponding to $E_T = 1$. However, one observation we can make from (27) is that since the absolute error tends to a constant in the limit $\Omega \to 0$ while the concentration $E[S]^{full}/\Omega$ tends to infinity, the relative error

$$\epsilon^{rel} = \frac{E[S]^{MM} - E[S]^{full}}{E[S]^{full}} \tag{13}$$

tends to zero. This is also the case in the large volume limit. Hence, the relative error will take a maximal value for some $\Omega > 0$. By maximising the relative error (13), we find that the maximum relative error

$$\epsilon^{rel}_{max} = \frac{\alpha^2 E_T}{4K_m V_{max}\mu} + \frac{\alpha}{4\mu} \tag{14}$$

occurs when

$$\Omega_{max} = \frac{2V_{max}\mu}{K_m V^2_{max} + E_T\alpha^2 + K_m V_{max}\mu}. \tag{15}$$

Given equations (14) and (15), we can ask whether there are conditions on the model parameters for which the maximum relative error will remain small independent of the system size Ω. The result (see Methods section 4.5) is that no such condition exists, since we arrive at the contradiction

$$1 << K_m\Omega_{max} \approx 1. \tag{16}$$

We note briefly that the first inequality in Eq. (16) resembles the condition (9), thus it makes sense that (16) does not hold because we would not expect to find the maximum error when the Michaelis-Menten approximation agrees nicely with the ODE. We can conclude that for every set of parameters, e^{rel}_{max} will be significant, i.e. the error due to the MM approximation will never be uniformly small in Ω. In what follows, we will elaborate on this and ask wether this error will be relevant under the same conditions for which the effects of molecular noise are significant.

2.4 MM error and stochastic focusing

In this section we will discuss two interesting questions for quantitative modelling; first, whether the error introduced by the MM approximation is significant under the same conditions for which the effects of noise in the system are significant, and second, if the volumes Ω for which the approximation is a substantial source of error represent relevant biological length scales. After all, elucidating the potential effects of noise is why we want to consider a stochastic model in the first place. To quantify the effects of noise we consider the stochastic focusing, here defined as the relative increase in the expected value of the substrate in the stochastic mass action (MA) model compared to the deterministic model

$$\delta_{SF} = \frac{E[S]^{full} - E[S]^{ODE}}{E[S]^{ODE}}. \tag{17}$$

It is clear from the above that in the small volume limit, $\delta_{SF} \to \infty$ and that in the large volume limit $\delta_{SF} \to 0$. Hence, by comparing δ_{SF} to ϵ^{rel} from Eq. (13), we can immediately conclude that in the small volume limit, the true stochastic effects will dominate over the error due to the MM approximation. In the large volume limit, both the error and the true effect of noise will be small.

An important question is what happens between these two limits: How large is the focusing effect for the system volume at which the error takes its maximal value? By plugging (15) into the definition (17), we find that $\delta_{SF}(\Omega_{max}) = 1$. That is, when the stochastic focusing effect results in a mean value which is double the ODE value the error is at its maximum and hence, by Eq. (32), significant. Fig. 3 shows an example of this behaviour for a representative set of biologically relevant parameters.

As can be seen in Fig. 3, the behaviour of the MM error and the true effect of noise can roughly be divided into three regions. First, to the far right, the relative error is much larger than the stochastic focusing effect, but both of those effects are very small. Here, all solutions are very close to the deterministic ODE solution. To the far left, the relative effect of stochastic focusing is much greater than the relative error due to MM. In between, we have a large range of volumes where the effect of stochastic focusing results in a significant

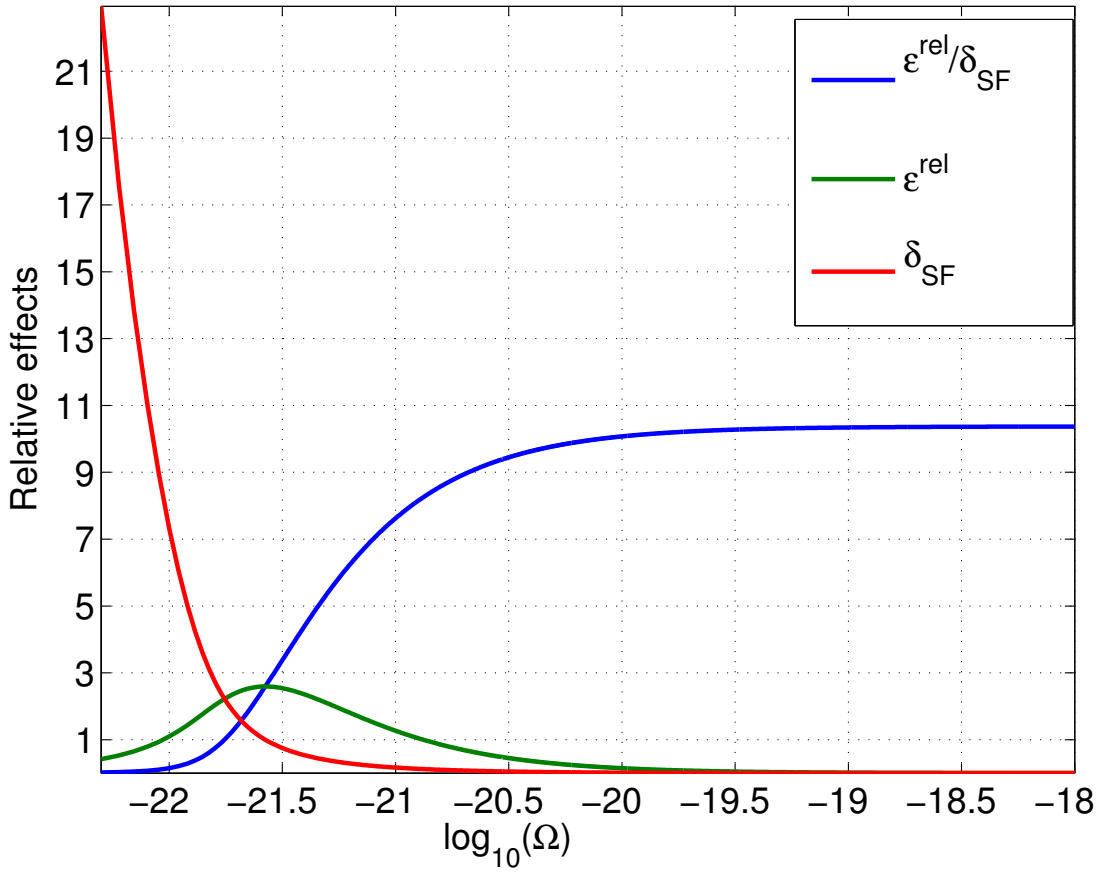

Figure 3: **Relative Error and Stochastic Focusing:** The relative effect of stochastic focusing δ_{SF} (red), the error introduced by the MM approximation ϵ^{rel} (green), and the quotient between them (blue). As can be seen, the behaviour can roughly be divided into three regions. First, to the far right, the relative error is much larger than the stochastic focusing effect, but both of those effects are very small. Here, all solutions are very close to the deterministic ODE solution. To the far left, the relative effect of stochastic focusing is much greater than the relative error due to MM. In between, we have a large range of volumes where the effect of stochastic focusing results in a significant deviation from the deterministic mean, but where the relative error due to MM is even greater. The parameters have been chosen to fall into biologically realistic ranges: $k_1 = 10^7 M^{-1}s^{-1}$, $k_2 = 0.1s^{-1}$, $k_3 = 10s^{-1}$, giving $K_m = 1.01 \times 10^{-6}M$. $E_T = 30^{-9}M$ (corresponding roughly to 20 molecules in $1\mu\text{m}^3$, which is roughly the volume of an *E. Coli* cell.)

deviation from the deterministic mean, but where the relative error due to MM is even greater. What are the length scales for which the MM error will cause unreliable simulations? As an example, consider the rightmost point where the volume is $1\mu m^3$, roughly the volume of an *E. Coli* cell. With the parameters as in the figure caption, a system of that size will contain approximately 20 enzyme molecules, a realistic number for many proteins in the living cell. As the figure shows, for this volume and these parameters the relative error (and also the stochastic focusing) is very small. However, for volumes less than $1 \times 10^{-21} m^3$ ($1000nm^3$), the MM error is substantial. This volume range would be relevant for reactions that become highly localised on a subcellular scale. A relevant example is the limited dispersion of mRNA in *E. Coli* [10], resulting in highly localised translational events.

For spatial stochastic models, where a subcellular resolution is introduced via a discretisation in subcompartments, this behaviour also results in numerical artefacts. This will be discussed in greater detail in the next section.

2.5 Michaelis-Menten, enzyme locality and the Reaction Diffusion Master Equation

In the modelling process, the next logical step in the refinement of the model beyond a well-mixed discrete stochastic setting is to consider a discrete spatial stochastic model. The results of the previous section show that when the reaction volume of a well-mixed system becomes small, the true effect of noise in the system becomes more pronounced but so does the error introduced by the MM approximation. As we will illustrate in this section, this is a point of great concern for spatial stochastic models in the RDME framework (see Methods section 4.6 for a brief description of the RDME).

In principle, the conversion of the stochastic well-mixed MM system (2) to a spatial stochastic model is straightforward; we simply use the propensity function (6) in each of the voxels, but with the total system volume Ω replaced by the local voxel volumes Ω_i. Apart from the shape of the domain (which is not important for the considerations here), the modeller has to select the voxel volumes. In this section, for notational simplicity and without loss of generality, we assume that the whole domain is of unit volume, $\Omega = 1$. We can then write the local (to voxels) MM propensity functions $a_{is}(S_i)$

$$a_{is} = \frac{V_{max} S_i}{K_m + S_i/\Omega_i}, \tag{18}$$

with S_i being the copy number of substrate in voxel $\mathcal{V}_i$.

Apart from the substrate and product which are diffusing in the domain, we need to specify how to handle the implicit enzyme species in the spatial model. In order to directly correspond to the well-mixed model reduction and to avoid reintroducing the enzyme explicitly, we are here regarding V_{max} as a given parameter of the model and assume that k_3 and E_T are not explicitly known. This means that the enzyme is considered globally (i.e. in the whole domain and not only in the voxels) uniformly distributed. As a consequence, we can effectively end up with fractions of enzyme molecules in the individual voxels. Clearly, this is not a realistic assumption for low enzyme densities, at least not in cases where there are reasons to believe that the spatial distribution of enzyme matters for the system dynamics [11]. Already in this light, it is questionable where MM kinetics should be applied in a spatial stochastic context in cases where the enzyme population is not macroscopically large.

In order to compare the results of spatial simulations with MM kinetics to simulations with the mass action (MA) model, we must decide how to treat the enzyme in the mass action model. Unlike in the well-mixed case, the models will no longer exactly correspond to each other if the enzyme is allowed to diffuse in the MA model. Hence, we first need to make assumptions to enforce a well-mixed enzyme in the mass action simulations. In principle, there are two ways we can achieve this. First, the enzyme can be made to be uniformly distributed over the voxels and prevented from diffusing, emulating a statically localised enzyme. Second, if the enzyme is diffusing freely with a large diffusion constant such that any reaction in which it participates is highly reaction limited, the enzyme can be considered effectively well-mixed in the global sense. The second scenario is in line with the usual and conventional interpretation of well-mixedness, while the first scenario corresponds precisely to the setting in the spatial MM model. Intuitively, it might be natural to think that both these scenarios should result in more or less the same simulation dynamics, but as we illustrate next, this is not the case.

Both scenarios are illustrated in Fig. 4, where we use the same total system size (unity) and parameters as in Fig. 1 and vary the diffusion constant of the substrate to range from very fast to very slow. As the diffusion constant of S decreases, both the MM (blue, cross) and MA (red,cross) systems approach the steady-state levels of a well-mixed system of volume equal to the voxel volume (dashed), rather than the volume of the whole simulation domain (solid). This can be understood from the results of the previous section, since in the limit of zero diffusion constant the global system effectively consists of K smaller, independent subsystems of size Ω_h. In the limit of fast diffusion, such that the substrate can also be considered well-mixed, the MA model approaches the well-mixed counterpart for the total system volume but the MM system does not. The parameter regime where a MM approximation of the system (1) in a spatial setting would be motivated from a biophysical perspective is to the far right of Fig. 4A, where the system is strongly reaction limited. However, even in this regime the RDME may not provide accurate simulations due to the artificial focusing effect demonstrated here.

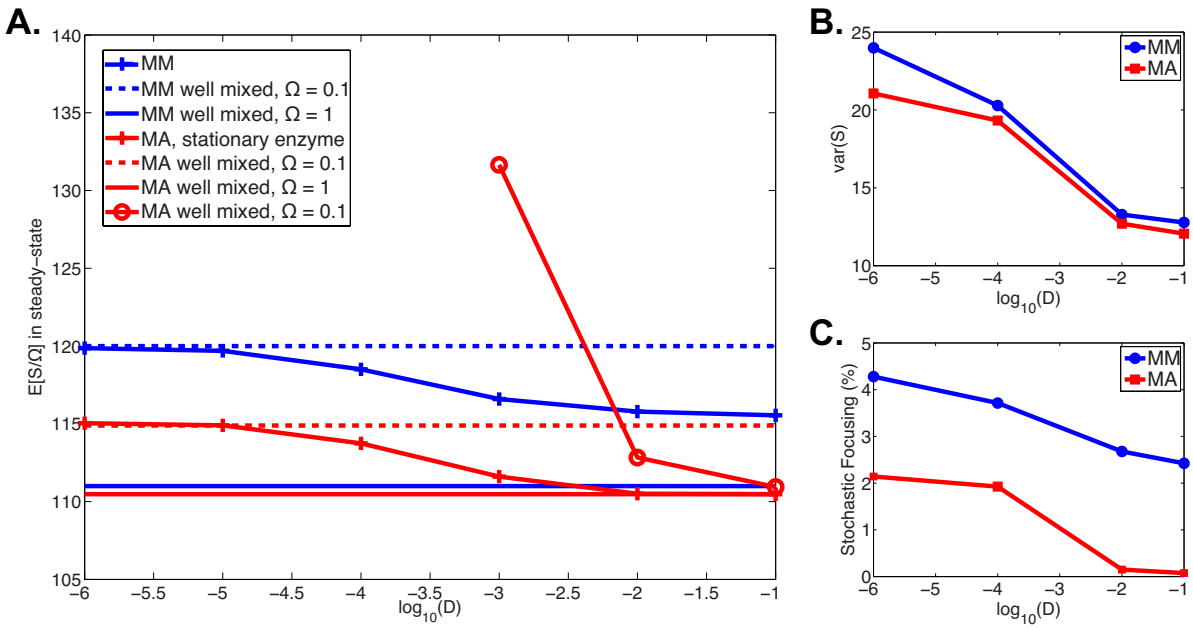

Figure 4: **Steady-state levels as a function of substrate mobility:** RDME simulations of MM and MA systems for the case where the enzyme in the MA systems is distributed uniformly over the voxels and is stationary. The mesh resolution is chosen such that there is an integer number of enzyme molecules in each voxel. **A:** As the diffusion constant becomes small, E[S/Ω] approaches the corresponding well-mixed value for the voxel volumes (dashed lines) from Fig. 1 for the MA (red, crosses) and MM (blue, crosses) systems respectively, rather than the value determined by the total system volume Ω (solid lines). This is to be expected because at zero diffusion each voxel become it's own independent well-mixed system, and the global sum of substrate molecules simply becomes the sum of those subsystems. Fast diffusion lowers the variance of S (**B**) by smoothing the reaction driven deviations from the mean in individual voxels. As Fig. 2 predicts, the reduction in variance shifts from lower reaction velocity (red diamond in Fig. 2) toward the zero variance limit (blue diamond in Fig. 2), resulting in reduced stochastic focusing (**C**, defined here as $100\frac{E[S]q(E[S])-E[Sq(S)]}{E[Sq(S)]}$). That is, up to a limit, diffusion reduces variability in the system and mitigates stochastic focusing.

For the case of a diffusing enzyme (red, circles), in the limit of slow diffusion $E[S/\Omega]$ diverges (only three points are shown in the figure for visualisation purposes). This is not caused by an artificial focusing effect, but rather by the locality effect discussed in [11]. S is still made constitutively across the domain, but P formation will be highly diffusion limited. The effect is that slow diffusion will result in long periods, on the time scale of S birth events, during which S in some voxels does not have access to E. The result is

that the growth of S checked only by its diffusion out of the voxel (which is also slow on the time scale of S birth events) until an E molecule diffuses in again. We note that this behaviour has nothing to do with the inaccuracies that can occur for small voxels and bimolecular reactions in mass action kinetics in the diffusion limited case [6, 8], since we conducted the simulations in Figs. 4 in 1D where those effects are not observed. What we demonstrate here would only be more pronounced in higher dimensions since the spurious focusing effect depends only on the voxel volumes.

We also note that diffusion can play a role in reducing the stochastic focusing effect by reducing the variance of S (Fig. 4B). In effect, diffusion is smoothing the spatial distribution of S by averaging between neighbouring voxels. This effect is limited by the noise induced by diffusion, and thus the variance will not converge to zero. Comparing Figs. 4 B and C makes it clear that this reduction in variance results in a clear reduction in stochastic focusing (defined here as $100\frac{E[S]q(E[S])-E[Sq(S)]}{E[Sq(S)]}$, note that at steady state $E[Sq(S)] = \frac{\Omega\mu}{V_{max}}$ in all cases) for both systems. This follows the intuition given in Fig. 2 that narrowing the distribution will reduce the stochastic focusing effect.

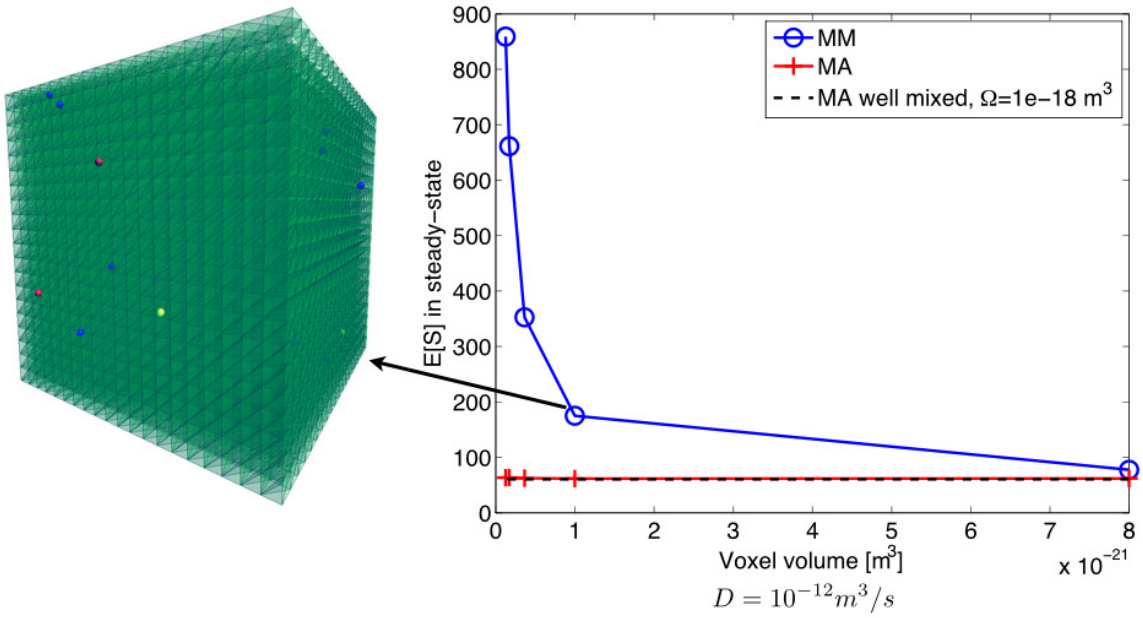

Figure 5: **Michaelis-Menten in 3D:** In 3D, the voxel volumes decrease quickly with the number of voxels, resulting in large errors when using the MM approximation. The figure shows simulations in 3D using the same parameters as in Fig. 3, and with $D = 10^{-12}m^2/s$. Diffusion is relatively fast and we would expect solutions close to the well mixed value (solid red) for all voxel sizes. This is indeed the case when using the MA system (red, cross) but the steady-state value of E[S] increases rapidly with decreasing voxel size for MM (blue, circles). The inset shows a snapshot of a simulation of the MA system using PyURDME (www.pyurdme.org), where the mesh is shown in green and the coloured spheres depicts S molecules (blue), E molecules (red) and ES complexes (yellow). The mesh resolution is here 20 voxels per axis, giving voxel volumes of $1.25 \times 10^{-21}m^3$, placing it in the far left region of volumes in Fig. 3.

In the well-mixed case and for biologically realistic parameters, the system volume for which the error introduced by the MM approximation becomes a pressing issue might be very small and may imply mean enzyme populations below unity. As an example, consider the parameter set in Fig. 3 where the rightmost point corresponds approximately to 20 enzyme molecules in $1\mu m^3$, roughly the volume of an *E. Coli* cell. As the figure implies, for some parameter sets, significant error will only be observed when we consider subcellular resolution. This is the aim of the RDME. Indeed, in a spatial stochastic simulation, we can quickly run into problematic volume regimes in individual voxels, leading to an artificial dependence on voxel

size. Fig. 5 illustrates this point. We simulate the MM and MA systems in a cube of volume $10^{-18}m^3$ (i.e. corresponding to the rightmost point in Fig. 3) in 3D using the same biologically realistic parameter values. We used a typical diffusion constant $D = 1\mu m^2/s$ for which the system is rather reaction limited. When varying the mesh resolution, the MA solution (red, cross) stays close to the well mixed solution (red, solid) for all voxel sizes, as expected. However, we see that the steady-state values of substrate are highly mesh dependent when using MM (blue,cross), with a large error even for modest mesh resolutions. The rightmost point corresponds to 5 voxels in each axis (a very coarse mesh) and the leftmost point to 20 voxels. So even though the error that would be incurred by MM in a well mixed simulation in the total system volume is small, by discretising space, the small volumes of the voxels result in a large error in the RDME solution. In fact, for these voxel sizes, we span the peak of the relative error in Fig. 3. Since the finer mesh resolutions would be necessary in order to resolve internal structures of the cells and to accurately resolve boundaries introduced by membranes, this greatly restricts the applicability of RDME simulations when the model contains MM motifs.

To further illustrate this point, we conclude by considering a model of a two stage MAPK pathway [7, 19]. The model definition and parameter values are found in Section 4.7. To illustrate the potential caveats of MM modelling, as a starting point we considered the parameter values used in [19]. For those values, the condition (5) is not strongly satisfied, and indeed, the authors rely on MA kinetics. However, small changes in parameters (no parameter is allowed to vary more than a factor of 10 from its original value, and they are only allowed to take biophysically plausible values), in line with what would be a minimal level of sensitivity analysis, result in a regime where the second step of the cascade appears amenable to MM model reduction (that is, condition 5 is satisfied). We note that when using the MM approximation it is essential to continually monitor the validity condition, however in this case it is always met and the result is not due to it's violation. Figure 6 shows the response of the system (the expected value of doubly phosphorylated $MAPKpp$) as a function of time when the cascade is simulated by the RDME in a cubic box of volume $1\mu m^3$. As can be seen, the MA and MM simulations agree well when there are only a small number of voxels (close to a well mixed system), but as the resolution increases, the MM system displays an artificial amplification over the MA system due to small-volume effects. These effects in the MM system could easily be misinterpreted as e.g. spatial effects caused from short-timscale spatiotemporal correlations (which in a MA system may need a high mesh resolution to be captured [19]).

3 Discussion

We have investigated the viability of progressing the Michaelis-Menten approximation from a well-mixed deterministic ODE model of enzyme kinetics to a well-mixed discrete stochastic model and finally to a spatial stochastic model. As we have shown, care must be exercised in interpreting effects of noise in the system if the MM approximation is used, since there will be ranges of volumes where the error introduced by the MM approximation will be significant in relation to the stochastic effects that would be observed using the full mass action model. Our analysis in the well mixed case provides a quantitative measure of the deviation from the MA solution, and shows that the error will be significant whenever the stochastic focusing effect in the substrate is significant. In fact, a small error implies that that both the stochastic MM and MA solutions are close to the deterministic solution.

What is clear from Fig. 4A is that there are two true contributions to amplification of E[S] above the deterministic level in spatial models with enzyme kinetics. The first contribution is illustrated when we assume that E is uniformly distributed and does not diffuse. This removes the issue of E not overlapping with location of creation of S. In this case there is still an issue of locality due to slow diffusion of substrate S, which becomes apparent as the diffusion coefficient goes to zero. In this limit small voxels are effectively isolated, thus voxel size becomes the effective system size. Not surprisingly, in this limit E[S/Ω] goes to the well-mixed equivalent for a system with volume equal to that of one of the voxels. This is the stochastic focusing effect, and in the limit of slow diffusion, the error due to the MM approximation can be understood quantitatively from the analysis in the previous section. However, we see that as the diffusion coefficient is increased there is a reduction in this focusing effect (Fig. 4C). This is because diffusion provides a smoothing or averaging between neighbours, and thus effectively narrows the distribution of S (Fig. 4B).

The second component to the spatial amplification is the locality effect discussed in [11]. In that work the authors introduce a system where a molecule S is created by another molecule X and degraded by an

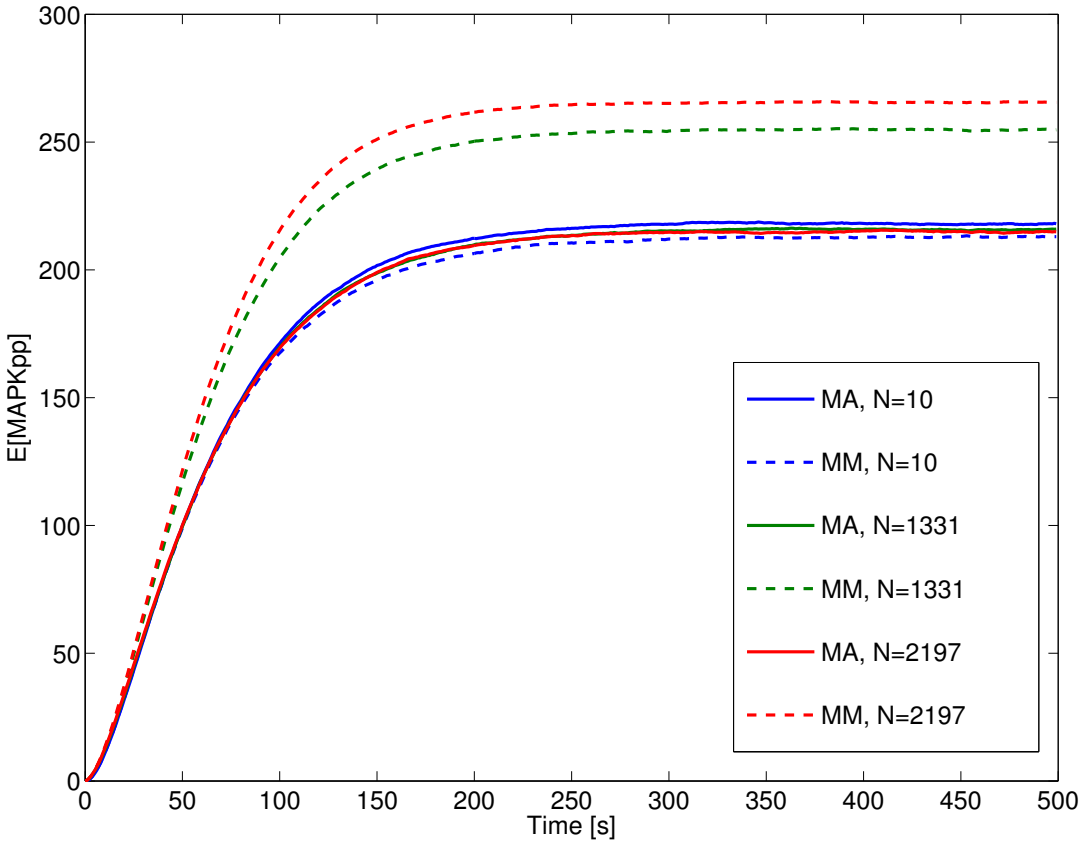

Figure 6: **Response of a two-stage MAPK cascade**: Small volume effects cause an artificial amplification of $MAPKpp$ in the stochastic MM system compared to the MA system for higher number of voxels in the mesh (dashed green and red lines). Here, the difference in steady-state levels between MA (solid lines) and MM is 23% for the finest mesh resolution, even though both models agree well for a close to well mixed system with only 10 voxels (blue lines). Had the comparison to a corresponding MA system not been available, this amplification could easily have been misinterpreted as spatial effects in the system, something that may need high spatiotemporal resolution to resolve [19].

enzyme E. They note that in the case of slow diffusion there will be situations where X and E molecules are not sufficiently close, causing "concentration peaks" around X and valleys around E molecules, resulting in slower effective degradation rates for S. In our system S is constitutively created everywhere thus as E is allowed to diffuse there will almost certainly be locations where there is no E around to convert S to P. The result is an explosion in S for slower diffusion coefficients, as shown in Fig. 4A. This effect can never be captured by a system using the naïve MM approximation. Apart from these difficulties, the fact that the accuracy of the MM solution depends so critically on the system volume means that it becomes highly sensitive to the mesh resolution in a RDME simulation, as illustrated in Fig. 5 and for the MAPK model in Fig 6.

In conclusion, our results paint a picture of the discrete stochastic MM approximation as being naturally applicable only in a well-mixed setting, and in that case only guaranteed to be accurate when the effects of noise (here defined as the stochastic focusing of the mean value) are small. Hence, while there are parameter regimes where the MM approximation gives accurate results, a deterministic simulation should be applicable, and preferable from a computational standpoint.

We note that another common approximation used frequently in systems biology to model, for example, cooperative binding of transcription factors to promoter regions is the Hill equation [14]:

$$\frac{[S]^n}{K_m^n + [S]^n}. \tag{19}$$

The Hill equation is understood as an approximation in the case of cooperative binding, where $max(n)$ is the number of possible binding events, and n takes that value only in the case of perfect cooperativity. Though it is awkward to talk about the cooperativity of one binding event, MM can be seen mathematically as a Hill equation with $n = 1$. The higher n, the stronger the nonlinearity, the steeper the curve and the greater the stochastic focusing effect. Therefore, the problems we have outlined for MM in both the well-mixed and spatial stochastic settings will likely be even more pronounced in models using the Hill equation.

As a final comment, in this paper we have considered the errors introduced by the MM model reduction in the mean value in steady state. That this error is small in cases where stochastic effects on the mean are relevant should be seen as a minimal requirement from a modelling perspective. If e.g. the error in variances is considered, even more stringent conditions than those discussed here may apply. As an example, in [20] it is shown that the error in the variance in steady state can be as large as 30% even in the regime where the stochastic MM, MA, and ODE solutions should result in the same mean values.

4 Methods

4.1 Ordinary Differential Equations

Denoting the concentration of S by $[S]$ (and similar for the other species), we write the reaction-rate ordinary differential equations (ODEs) for the mass action system (1)

$$\begin{aligned}
\frac{d[S]}{dt} &= \mu - k_1[S]([E_T] - [ES]) + k_2[ES] \\
\frac{d[ES]}{dt} &= k_1[S]([E_T] - [ES]) - k_2[ES] - k_3[ES] \\
\frac{d[P]}{dt} &= k_3[ES] - k_d[P].
\end{aligned} \tag{20}$$

For the Michaelis-Menten system (2) we have

$$\begin{aligned}
\frac{d[S]}{dt} &= \mu - \frac{V_{max}[S]}{Km + [S]} \\
\frac{d[P]}{dt} &= \frac{V_{max}[S]}{Km + [S]} - k_d[P].
\end{aligned} \tag{21}$$

4.2 The Chemical Master Equation

The discrete stochastic model uses the continuous-time discrete-space Markov process framework, and thus its probability density function obeys the forward Kolmogorov equations. In the case of chemical kinetics, the specific form is the Chemical Master Equation (CME). The population of each of the N molecular species in the system at time t is defined by the population vector $\mathbf{x}(t) = [x_1(t)...x_N(t)]$, where $x_i(t)$ gives the population of species i at time t. The chemical species react through R reaction channels, each with an associated stoichiometry vector ν_r, such that if reaction r fires at time $t+\tau$ the populations are updated by $\mathbf{x}(\mathbf{t}+\tau) = \mathbf{x}(\mathbf{t}) + \nu_r$. Each reaction also has an associated propensity $a_r(\mathbf{x}(t))$, such that the probability of reaction r firing in the next infinitesimal time interval $[t, t+dt]$ is $a_r(\mathbf{x}(t))dt$. The evolution of the probability of being in a given state $\mathbf{x}$ is then given by

$$\frac{dP(\mathbf{x},t)}{dt} = \sum_{r=1}^{R} a_r(\mathbf{x}-\nu_r)P(\mathbf{x}-\nu_r,t) - \sum_{r=1}^{R} a_r(\mathbf{x})P(\mathbf{x},t). \tag{22}$$

A derivation of the CME can be found in [3]. Sample trajectories can be obtained using the Stochastic Simulation Algorithm (SSA) [2], and an ensemble of such trajectories can be used to approximate the solution to the CME.

4.3 Moment Equations

By expanding the moments to second order central moments and closing by setting third order and higher moments to zero [1], we obtain the following approximate equations for the fist and second moments for the MM model:

$$\begin{aligned}
\frac{dE[S]}{dt} =& \mu\Omega - \frac{V_{max}E[S]}{K_m + E[S]/\Omega} - \frac{E[S]V_{max}\sigma^2[S]}{\Omega^2(K_m+E[S]/\Omega)^3} + \frac{V_{max}\sigma^2[S]}{\Omega(K_m+E[S]/\Omega)^2} \\
\frac{d\sigma^2[S]}{dt} =& \mu\Omega + \frac{V_{max}E[S]}{K_m + E[S]/\Omega} + \frac{E[S]V_{max}\sigma^2[S]}{\Omega^2(K_m+E[S]/\Omega)^3} - \frac{V_{max}\sigma^2[S]}{\Omega(K_m+E[S]/\Omega)^2} + \frac{2E[S]V_{max}\sigma^2[S]}{\Omega(K_m+E[S]/\Omega)^2} \\
& - \frac{2V_{max}\sigma^2[S]}{K_m+E[S]/\Omega}
\end{aligned} \tag{23}$$

Moment equations for MA system:

$$\begin{aligned}
\frac{dE[S]}{dt} =& \mu\Omega + k_2E_t\Omega - k_2E[E] - \frac{k_1}{\Omega}E[E]E[S] - \frac{k_1}{\Omega}\text{cov[ES]} \\
\frac{dE[E]}{dt} =& (k_2+k_3)E_t\Omega - (k_2+k_3)E[E] - \frac{k_1}{\Omega}E[E]E[S] - \frac{k_1}{\Omega}\text{cov[ES]} \\
\frac{d\sigma^2[S]}{dt} =& \mu\Omega + k_2E_t\Omega - k_2E[E] + \frac{k_1}{\Omega}E[E]E[S] - \left(2k_2 - \frac{k_1}{\Omega} + \frac{2k_1E[S]}{\Omega}\right)\text{cov[ES]} - \frac{2k_1E[E]}{\Omega}\sigma^2[S] \\
\frac{d\sigma^2[E]}{dt} =& (k_2+k_3)E_t\Omega - (k_2+k_3)E[E] + \frac{k_1}{\Omega}E[E]E[S] + \left(\frac{k_1}{\Omega} - \frac{2k_1E[E]}{\Omega}\right)\text{cov[ES]} - \left(2k_2+2k_3+\frac{2k_1E[S]}{\Omega}\right)\sigma^2[E] \\
\frac{d\text{cov[ES]}}{dt} =& k_2E_t\Omega - k_2E[E] + \frac{k_1}{\Omega}E[E]E[S] - \left(k_2+k_3-\frac{k_1}{\Omega}+\frac{k_1E[E]}{\Omega}+\frac{k_1E[S]}{\Omega}\right)\text{cov[ES]} - \frac{k_1E[E]}{\Omega}\sigma^2[S] \\
& - \left(k_2+\frac{k_1E[S]}{\Omega}\right)\sigma^2[E]
\end{aligned} \tag{24}$$

4.4 Small Volume Limit

In the small volume limit $\Omega \to 0$, we can expand (10) around Ω in a Taylor series and truncate higher order terms to obtain

$$E[S]^{full} = \Omega\frac{\mu K_m}{\alpha} + \frac{\mu}{\alpha} - \Omega\frac{\alpha E_T}{V_{max}} - \Omega K_m + \mathcal{O}(\Omega^2). \tag{25}$$

For the error in the small volume limit we thus obtain

$$\epsilon_{\Omega\to 0} = E_T(1 - \frac{\mu}{V_{max}}) + K_m. \tag{26}$$

At steady state $\mu = k_3 ES = (E_T - E)k_3 = V_{max} - k_3 E$, thus Equation (26) becomes:

$$\epsilon_{\Omega\to 0} = E_T(1 - \frac{V_{max} + k_3 E}{V_{max}}) + K_m = E + K_m \approx K_m, \tag{27}$$

since $(1 - \mu/V_{max}) \in (0, 1)$ and $E_T << K_m$ under the assumption (5). While (27) offers some insight into the behaviour of the error, the Taylor series converges slowly. Even for the smallest volumes in Fig. 1 we are far from the asymptotic regime.

4.5 Maximum Error

We can rearrange (14) and (15) to obtain

$$\Omega_{max} = \frac{1}{K_m} \cdot \frac{1}{1 + 2\epsilon^{rel}_{max}} \tag{28}$$

or equivalently

$$\epsilon^{rel}_{max} = \left(\frac{1}{K_m \Omega_{max}} - 1 \right) /2. \tag{29}$$

Now, to enforce a small relative error we require that

$$e^{rel}_{max} << 1. \tag{30}$$

When applied to Eq. (28) this condition implies that

$$\Omega_{max} K_m \approx 1. \tag{31}$$

Plugging equations (30) and (31) into Eq. (29) results in the contradictory condition that

$$1 << K_m \Omega_{max} \approx 1. \tag{32}$$

4.6 The Reaction Diffusion Master Equation

The approach of the RDME is to divide space into voxels, such that each voxel can be assumed to be well-mixed in the sense of satisfying the conditions for the CME. Diffusion is then handled as first order events similar to a death event in the originating voxel and a birth event in the destination voxel. More precisely, let the domain be divided into K non-overlapping voxels $\mathcal{V}_i, i = 1 \dots K$, each of volume Ω_i [21]. The state of the system is now the random vector $\mathbf{S} = (S_1, ..., S_i, ...S_K)$ where S_i is the discrete number of molecules in $\mathcal{V}_i$. Inside individual voxels, the molecules react according to the same rules that govern a well-mixed system, but now confined to the smaller, local volume. Diffusion is modeled as jump events that move molecules between adjacent voxels. For a Cartesian grid with mesh spacing h, the rate for a diffusive jump $S_i \to S_j$ is given by D/h^2, where D is the diffusion constant. An example of a mesh and a snapshot of a simulation in 3D is shown in Fig. 5.

4.7 MAPK model

This model represents two steps of a MAPK phosphorylation cascade. It is based on the model in [19], where also a reactivation and activation step of the enzymes $MAPKK$ and P is considered. Here, we have assumed that the reactivation steps are fast, to arrive at a model on Michaelis-Menten format, in line with other larger models of the cascade such as the classical model by Huang and Ferrel [7].

The mass action model is expressed as:

$$MAPK + MAPKK \underset{k_2}{\overset{k_1}{\rightleftarrows}} MAPK\_MAPKK \xrightarrow{k_3} MAPKK + MAPK_p \tag{33}$$

$$MAPK_p + MAPKK \underset{k_5}{\overset{k_4}{\rightleftarrows}} MAPK_p\_MAPKK \xrightarrow{k_6} MAPKK + MAPK_{pp} \tag{34}$$

$$MAPK_{pp} + P \underset{k_8}{\overset{k_7}{\rightleftarrows}} MAPK_{pp}\_P \xrightarrow{k_9} P + MAPK_p \tag{35}$$

$$MAPK_p + P \underset{k_{11}}{\overset{k_{10}}{\rightleftarrows}} MAPK_p\_P \xrightarrow{k_{12}} P + MAPK \tag{36}$$

with parameters $k_1 = k_7 = 2.6 \times 10^6 M^{-1}s^{-1}$, $k_4 = k_{10} = 5.6 \times 10^6 M^{-1}s^{-1}$, $k_2 = 1.35s^{-1}$, $k_3 = 1.5s^{-1}$, $k_5 = 1.73s^{-1}$, $k_5 = 1.5s^{-1}$, $k_8 = 5.35s^{-1}$,$k_9 = 1.5s^{-1}$,$k_{11} = 5.73s^{-1}$ and $k_{12} = 1.73s^{-1}$. The initial concentrations of enzyme is $[MAPK] = 500nM$, $[MAPKK] = 25nM$ and $[P] = 25nM$.

The Michaelis-Menten version of the model is given by

$$V^{(1)}_{max} = k_9[P], K^{(1)}_m = (k_8 + k_9)/k_7 \tag{37}$$

$$V^{(2)}_{max} = k_{12}[P], K^{(2)}_m = (k_{11} + k_{12})/k_{10} \tag{38}$$

$$\tag{39}$$

$$MAPK + MAPKK \underset{k_2}{\overset{k1}{\rightleftarrows}} MAPK\_MAPKK \xrightarrow{k_3} MAPKK + MAPK_p \tag{40}$$

$$MAPK_p + MAPKK \underset{k_5}{\overset{k4}{\rightleftarrows}} MAPK_p\_MAPKK \xrightarrow{k_6} MAPKK + MAPK_{pp} \tag{41}$$

$$MAPK_{pp} \xrightarrow{\frac{V^{(1)}_{max} MAPK_{pp}}{K^{(1)}_m + MAPK_{pp}}} MAPK_p \tag{42}$$

$$MAPK_p \xrightarrow{\frac{V^{(2)}_{max} MAPK_p}{K^{(2)}_m + MAPK_p}} MAPK \tag{43}$$

5 Data Accessibility

Simulations have been conducted using the pyURDME software. It is publicly available from www.pyurdme.org.

6 Competing Interests

We have no competing interests

7 Author Contributions

MJL and AH designed and performed the research. MJL, LP and AH analysed data and wrote the paper.

8 Funding

This work was funded by National Science Foundation (NSF) Award No. DMS-1001012, ICB Award No. W911NF-09-0001 from the U.S. Army Research Office, NIBIB of the NIH under Award No. R01-EB014877-01, and (U.S.) Department of Energy (DOE) Award No. DE-SC0008975. The content of this paper is solely the responsibility of the authors and does not necessarily represent the official views of these agencies.

References

[1] Engblom, S. 2006 Computing the moments of high dimensional solutions of the master equation. *Appl. Math. Comput.*, **180**(2), 498–515.

[2] Gillespie, D. T. 1977 Exact stochastic simulation of coupled chemical reactions. *The Journal of Physical Chemistry*, **81**(25), 2340–2361.

[3] Gillespie, D. T. 1992 A rigorous derivation of the chemical master equation. *Physica A: Statistical Mechanics and its Applications*, **188**(1-3), 404 – 425.

[4] Gillespie, D. T., Hellander, A. & Petzold, L. R. 2013 Perspective: Stochastic algorithms for chemical kinetics. *The Journal of Chemical Physics*, **138**(17), 170901. (doi:http://dx.doi.org/10.1063/1.4801941)

[5] Grima, R. 2009 Noise-induced breakdown of the Michaelis-Menten equation in steady-state conditions. *Phys. Rev. Lett.*, **102**(218103).

[6] Hellander, S., Hellander, A. & Petzold, L. 2012 The reaction-diffusion master equation in the microscopic limit. *Phys. Rev. E*, **85**(4), 042 901.

[7] Huang, C. Y. & Ferrell, J. E. 1996 Ultrasensitivity in the mitogen-activated protein kinase cascade. *Proceedings of the National Academy of Sciences*, **93**(19), 10 078–10 083.

[8] Isaacson, S. A. 2009 The reaction-diffusion master equation as an asymptotic approximation of diffusion to a small target. *SIAM J. Appl. Math.*, **70**, 77–111.

[9] Kim, J. K., Josić, K. & Bennett, M. R. 2014 The validity of quasi steady-state approximations in discrete stochastic simulations. *arXiv preprint arXiv:1406.2244*.

[10] Llopis, P. M., Jackson, A. F., Sliusarenko, O., Surovtsev, I., Heinritz, J., Emonet, T. & Jacobs-Wagner, C. 2010 Spatial organization of the flow of genetic information in bacteria. *Nature*, **466**(7302), 77–81.

[11] Mahmutovic, A., Fange, D., Berg, O. G. & Elf, J. 2012 Lost in presumption: stochastic reactions in spatial models. *Nature methods*, **9**(12), 1163–1166.

[12] Mastny, E. A., Haseltine, E. L. & Rawlings, J. B. 2007 Two classes of quasi-steady-state model reductions for stochastic kinetics. *The Journal of Chemical Physics*, **127**(9), 094106. (doi: http://dx.doi.org/10.1063/1.2764480)

[13] Michaelis, L. & Menten, M. L. 1913 Die kinetik der invertinwirkung. *Biochem. z*, **49**(333-369), 352.

[14] Nelson, D. L., Lehninger, A. L. & Cox, M. M. 2008 *Lehninger principles of biochemistry*. Macmillan.

[15] Paulsson, J., Berg, O. G. & Ehrenberg, M. 2000 Stochastic focusing: Fluctuation-enhanced sensitivity of intracellular regulation. *Proc. Nat. Acad. Sci. USA*, **97**(13), 7148–7153.

[16] Rao, C. V. & Arkin, A. 2003 Stochastic chemical kinetics and the quasi-steady state assumption: Application to the Gillespie algorithm. *J. Chem. Phys.*, **118**(11), 4999–5010.

[17] Sanft, K., Gillespie, D. T. & Petzold, L. R. 2011 Legitimacy of the stochastic Michaelis-Menten assumption. *IET Syst. Biol.*, **5**(1), 58–69.

[18] Segel, L. A. & Slemrod, M. 1989 The quasi-steady-state assumption: A case study in perturbation. *SIAM Review*, **31**(3), 446–477.

[19] Takahashi, K., T?nase-Nicola, S. & ten Wolde, P. R. 2010 Spatio-temporal correlations can drastically change the response of a mapk pathway. *Proceedings of the National Academy of Sciences*, **107**(6), 2473–2478. (doi:10.1073/pnas.0906885107)

[20] Thomas, P., Straube, A. V. & Grima, R. 2011 Communication: Limitations of the stochastic quasi-steady-state approximation in open biochemical reaction networks. *The Journal of Chemical Physics*, **135**(18), 181103. (doi:http://dx.doi.org/10.1063/1.3661156)

[21] van Kampen, N. G. 2007 *Stochastic Processes in Physics and Chemistry*. Elsevier, 3rd edn.

[22] Wu, S., Fu, J., Cao, Y. & Petzold, L. 2011 Michaelis–Menten speeds up tau-leaping under a wide range of conditions. *The Journal of Chemical Physics*, **134**(13), 134112. (doi: http://dx.doi.org/10.1063/1.3576123)

List of Figures

List of Tables